BENHA MEDICAL JOURNAL bmj

Print ISSN 1110-208X

Online ISSN 2357-0016

Original article

Assessment of (EZH2) Expression, Digital Image Analysis of CD8+ Lymphocytes, and Automated Nuclear Morphometry in Renal Cell Carcinoma

Eman M. Said, Ranih Z. Amer, Sara A. Madkour, Marwa S. Abd Allah

Department of anatomic Pathology, Faculty of Medicine Benha University, Egypt.

Corresponding to: Sara A. Madkour, Department of anatomic Pathology, Faculty of Medicine Benha University, Egypt.

Email:

sara.madkour@fmed.bu.edu

Received: 22 June 2024

Accepted:9 September 2024

Abstract

Background: The enhancer of zeste homolog-2 is overexpressed in many human cancers. High CD8+ T cell density was associated with favorable prognosis in various tumors, but this isn't true for all cancers. Nuclear grading of RCC is an important prognostic factor but it is subjective. Automated nuclear morphometry is more accurate. **Aim:** Evaluation of EZH2 expression, CD8+ density, and nuclear morphometry in RCC. **Methods:** In this retrospective study, IHC staining of EZH2 and CD8+ was done and assessed for each RCC case. CD8+ density was calculated. Quantitative nuclear morphometry was done by automated image analysis. **Results:** EZH2 expression showed highly significant relation with histologic grade(P=0.002), and AJCC stage(P=0.004)& showed significant relation with tumor extent(P=0.012), nodal metastasis (P=0.033), and distant metastasis(P=0.044). Highly significant relation between CD8+ density and histologic types(P=0.0001), histologic grade (P<0.001), tumor extent(P=0.0002), nodal metastasis(P=0.003), and AJCC stage(P=0.001). Both EZH2 and CD8+ density showed highly significant relation with OS(P=0.008 &0.001 respectively) and DFS(P<0.001 &0.001 respectively). MNA, MNP, MN long and short axis had high significant relation with histologic grade(P<0.001, for each), tumor extent(P=0.001, 0.001, 0.001 & 0.002 respectively), CD8+ density(P <0.001, for each), OS(P<0.001, for each) and DFS (P=0.003, 0.006, 0.003 & 0.002 respectively), and had significant relation with nodal metastasis (P=0.044, 0.027, 0.032 & 0.038 respectively), distant metastasis (P=0.049, 0.047, 0.036, and 0.037 respectively), AJCC stage group (P= .011, 0.013, 0.022, and 0.009 respectively), EZH2 expression(P=0.011, 0.013, 0.006 & 0.027 respectively). **Conclusion:** EZH2, CD8+ density and nuclear morphometry could be reliable prognostic factors in RCC.

Key words: Renal cell carcinoma, EZH2, CD8+, Nuclear morphometry, image analysis.

Abbreviations

Enhancer of zeste homolog-2 (EZH2) , Renal cell carcinoma (RCC), Polycomb repressive complex 2 (PRC2), The American Joint Committee on Cancer (AJCC), The International Society of Urological Pathology (ISUP), Disease-

free survival (DFS), Overall survival (OS), Clear cell RCC (CCRCC), Tumor infiltrating lymphocytes (TILs), Papillary RCC (PRCC), Chromophobe RCC (ChRCC), Mean nuclear area (MNA), Mean nuclear perimeter (MNP).

Introduction

Renal cell carcinoma (RCC) is the most common urological malignancy, accounting for 90% of all kidney cancer cases. [1] It is the twelfth most common cancer worldwide. In Egypt, RCC ranks the 14th regarding both incidence and mortality [2]. Clear cell RCC (CCRCC) is the most common histologic RCC type representing about 75% of the cases. Papillary and chromophobe types are the most common non-CCRCC histologic types accounting for 13–20% and 5–7% of RCC cases, respectively [3]. Several potential biomarkers are currently being investigated to detect the risk of RCC progression and recurrence, aiming to guide therapy. But no definitive marker is yet validated.

Enhancer of zeste homolog 2 (EZH2) is the enzymatic subunit of Polycomb repressive complex 2 (PRC2). This complex that methylates lysine 27 of histone H3 (H3K27) promoting transcriptional silencing of various genes [4]. EZH2 also methylates non-histone protein substrates [5]. EZH2 could activate downstream genes by direct methylation of non-histone proteins. [6]. So, EZH2 works as a master regulator of cell cycle progression, autophagy, and apoptosis, DNA repair [7].

Enhancer of zeste homolog 2 is required for cancer cell proliferation, migration, invasion, and epithelial-mesenchymal transition [8]. EZH2 dysregulations were described in many human cancers and has become a potential target for cancer therapy [9].

CD8+ cytotoxic T cells is one of the key tumor-antagonizing immune cells [10]. High levels of tumor infiltrating CD8+ T cells were associated with favorable prognosis in many cancers. In the context of RCC, the role of cytotoxic CD8+ TILs has been controversial. This discrepancy needs to be further studied [11].

The nuclear grade of RCC is an important prognostic factors determining the patient survival [12]. Subjectivity in nuclear grading highlights the need for more objective methods, such as the quantitative assessment of nuclear morphometry with computer imaging systems [13].

Methods

This retrospective study was carried out on 55 formalin fixed paraffin embedded blocks of RCC, obtained from the Pathology Department, Faculty of Medicine-Benha University, Egypt (during the years from March 2014 to November 2020). Ten tissue blocks of normal renal tissue were used as a control group. The study was approved by the Ethical Committee of faculty of Medicine, Benha University number (MD 14-1-2022). Clinicopathological data of studied cases were obtained from patients' files. The follow-up period ranged from 9-36 months. **Overall survival** was the number of months from date of diagnosis to date of death. **Disease-free survival** was the number of months from date

of diagnosis until date of recurrence or metastasis.

Hematoxylin and Eosin stain:

Hematoxylin and eosin-stained slides from each case were reviewed for pathological evaluation for reviewing diagnosis, histologic typing, and nuclear grading and also to be used for image analysis. At this review, blocks were selected for immunohistochemistry.

Immunohistochemical method:

Four-micron tissue sections were obtained from tissue blocks on positive charged slides. After xylene deparaffinization, sections were rehydrated in descending grades of alcohol then in distilled water. Antigen retrieval was performed by using 10 mmol/L citrate monohydrate buffer (PH 6.0). Sections were incubated with diluted primary EZH2 antibody ***(Rabbit monoclonal antibody, 0.1mg/ml concentration, Chongqing Biospes company, Cat. YMA1231, conc. China)*** and CD8+ antibody ***(Rabbit polyclonal antibody, 0.1mg/ml concentration, Chongqing Biospes company, Cat. # BPA1021, conc. China),*** diluted at 1:50 overnight. A conventional labelled streptavidin-biotin system was used for immunodetection ***(Dako Cytomation, Denmark, A/S)*.** Immunoreaction was visualized by adding DAB chromogen. Counterstaining was performed with the Mayer hematoxylin.

Histologic sections from normal testicular tissue were used as positive controls for EZH2 antibody[14]**.** Histologic sections from tonsil were used as positive controls for CD8 antibody[15]**.** For negative control the primary antibody was omitted from the staining procedure.

Interpretation of EZH2 immunohistochemical staining:

EZH2 expression was detected as nuclear brown coloration in malignant cells. Immunoreactivity was assessed by evaluating extent and intensity of stained nuclei. Intensity was scored as(0,1,2,3). Extent of staining was grouped as 0 for < 5% positive cells, 1 for 5% to 25% positive cells, 2 for 26% to 50% positive cells, and 3 for > 50% positive cells. Final score was calculated by multiplying extent score with intensity score. Cases were subdivided into **Negative**; a score of 0, **Weak expression**; score 1 up to 4, **Strong expression**; score 5 up to 9 [16].

Interpretation and Calculation of CD8+ density:

CD8+ expression was detected as membranous brownish coloration of lymphocytes among tumor epithelial cells and stroma.

Digital images of CD8-stained slides were analyzed using **ImageJ software, version 1.54g** [17]**.** According to previous published protocol[18] **,** images were processed to determine number of CD8+ cells in each tissue spot and to measure the corresponding exact area of this tissue spot. Number of stained cells and the area in square millimeters of each individual spot was used to calculate density of stained cells/ mm^2 (number of cells per square mm). The median value was used as a cut-off point to categorize cases into CD8+ high, and CD8+ low cases [19].

Automated Nuclear morphometry:

Representative images of highest-grade tumor areas from H&E stained slides of RCC were taken using x40 magnification. Like a published algorithm,[20] we did nuclear segmentation. The "**analyze tool**" in **ImageJ** was configured to measure nuclear area, perimeter, circularity, long and short axis.

Statistical analysis:

Categorical data were presented as number and percentages while quantitative data were expressed as mean ±standard deviation (SD). Chi square test ($\chi 2$), or Fisher's exact test were used to analyze categorical variables. Quantitative data were tested for normality using Shapiro-Wilks test, then using Student "t" test if normally distributed, or Man-Whitney U test and Kruskal-Wallis test if not normally distributed for analyzing difference. Spearman's test was used for correlation. Kaplan–Meierr curve were used to calculate survival using the log-rank test. The significance is judged at the (<0.05) level. P-value ≤0.01 is considered highly significant. P-value >0.01 is considered non-significant Statistical analysis was performed using SPSS version 22 **(SPSS Inc, Chicago, IL, USA).**

Results:

Clinicopathological results are shown in Table (1)

EZH2 expression: There was a highly significant relation between EZH2 expression and histologic grade (P=0.002), AJCC stage group(P=0.004), OS (P=0.008), and DFS(P <0.001). There was a significant relation between EZH2 expression and tumor extent (P=0.012), nodal metastasis (P= 0.033), and distant metastasis in studied cases (P=0.044). No significant relation was found between EZH2 expression and histologic types in studied cases (P=0.731) (Table 2)(Figure 1).

CD8 density: Median CD8+ density (184 cells/mm2) was used as a cut-off point to categorize studied cases into CD8+ high, and CD8+ low density. There was high significant relation between CD8+ lymphocytes density score and RCC histologic types(P= 0.0001), histologic grade (P<0.001), tumor extent (P= 0.0002),nodal metastasis (P=0.003), AJCC stage group(P= 0.001), OS and DFS (P=0.001, for each) in studied cases. There was no significant relation between CD8+ density and distant metastasis in studied RCC cases (P=0.311). (Table 3) (Figure 2-3).

There was a highly significant relation between EZH2 expression and CD8+ density in studied cases(P= 0.005). We divided RCC cases into 6 groups according to EZH2 expression and CD8+ density (Table 4). The different groups of combined EZH2 expression and CD8 density showed significant relation with OS(P=0.015), and highly significant relation with the DFS(P<0.001). Negative EZH2 /Low CD8+ density group was associated with the most prolonged OS and DFS than other groups (36 months, for each). (Figure 5&6)

Nuclear morphometry: As shown in (Tables 5-6) &(Figure 4), The MNA, MNP, mean nuclear long axis and mean nuclear short axis showed highly significant relation

with the histologic grade (P<0.001, for each), and tumor extent (P= 0.001, 0.001, 0.001, and 0.002 respectively), and significant relation with nodal metastasis (P= 0.044, 0.027, 0.032, and 0.038 respectively), distant metastasis (P= 0.049, 0.047, 0.036, and 0.037 respectively), and AJCC stage group (P= 0.011, 0.013, 0.022, and 0.009 respectively). Mean nuclear circularity showed high significant relation with histologic grade (P= 0.006). There was a significant statistical relation between EZH2 expression and MNA (P= 0.011), MNP (P= 0.013), and mean nuclear short axis (P= 0.027), and highly significant statistical relation with the mean nuclear long axis (P= 0.006).

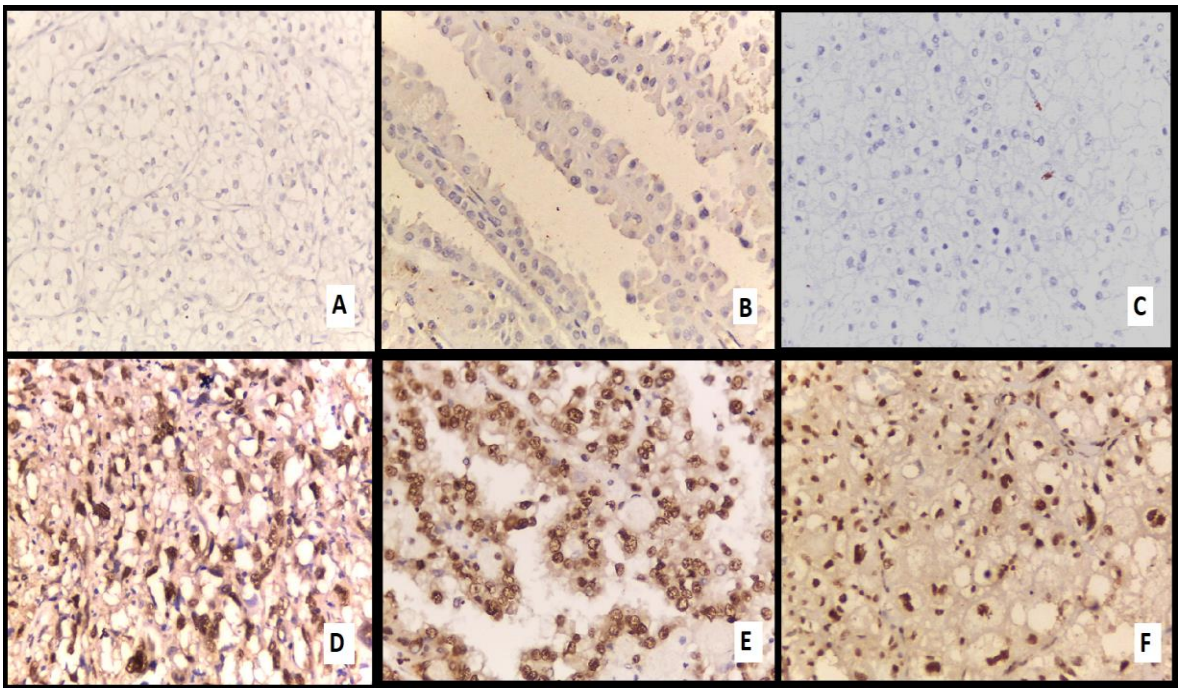

Figure (1): (A) Clear cell RCC, Grade 1 with negative nuclear EZH2 expression. (ABC, x400), (B) Papillary RCC, Grade 1 with negative nuclear EZH2 expression. (ABC, x400). (C) Chromophobe RCC, Grade 1 with negative nuclear EZH2 expression. (ABC, x400), (D) Chromophobe RCC, Grade 3 with strong nuclear EZH2 expression. (ABC, x400)., (E) Papillary RCC, Grade 3 with strong nuclear EZH2 expression. (ABC, x400)., (F) Chromophobe RCC, Grade 3 with strong nuclear EZH2 expression. (ABC, x400).

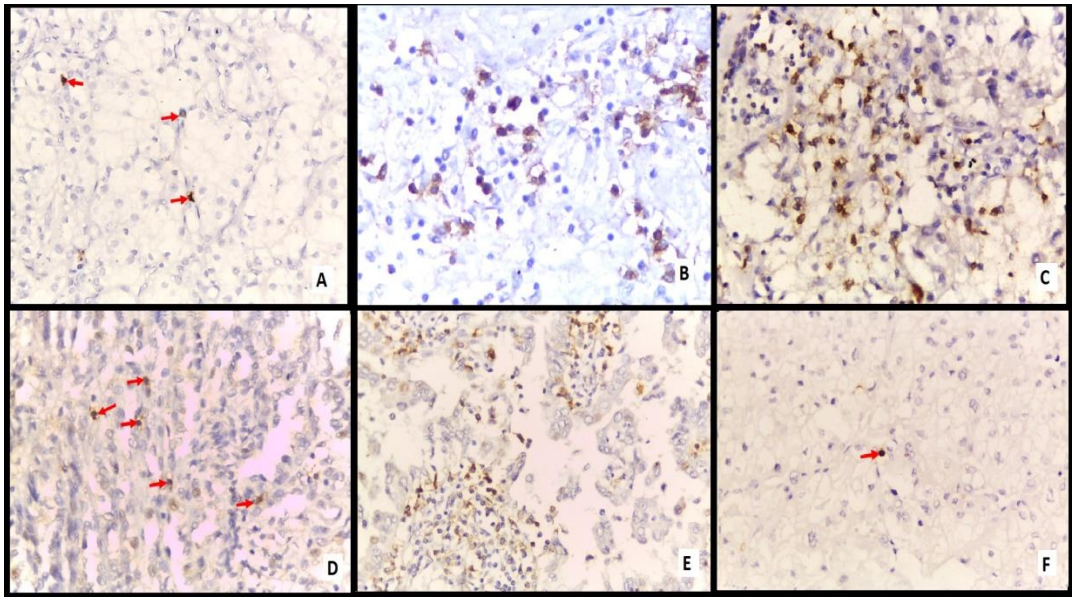

Figure (2): (A) Clear cell RCC, Grade 1 with low CD8+ density (ABC, x200), inset (ABC, x400). , (B) Clear cell RCC, Grade 2 with high CD8+ density. (ABC, x400). , (C) Clear cell RCC, Grade 3 with high CD8+ density (ABC, x400). , (D) Papillary RCC, Grade 2 with low CD8+ density (ABC, x400). , (E) Papillary RCC, Grade 3 with high CD8+ density (ABC, x400). , (F) Chromophobe RCC, Grade 2 with low CD8+ density (ABC, x400).

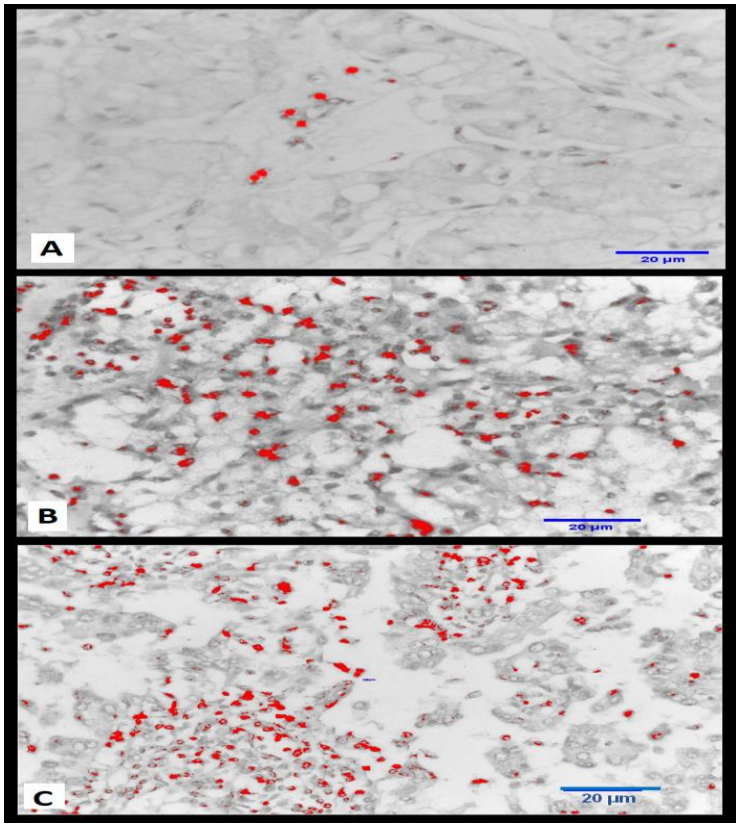

Figure 3: Quantification of CD8+ cells by ImageJ Analysis (recognized as red color), in (A) clear cell RCC grade 1 with low CD8+ density (100 cells/mm2), (ABC, x400) , (B) in clear cell RCC grade 3 with high CD8+ density (775 cells/mm2), (ABC, x400), (C) in papillary RCC grade 3 with high CD8+ density (515 cells/mm2), (ABC, x400).

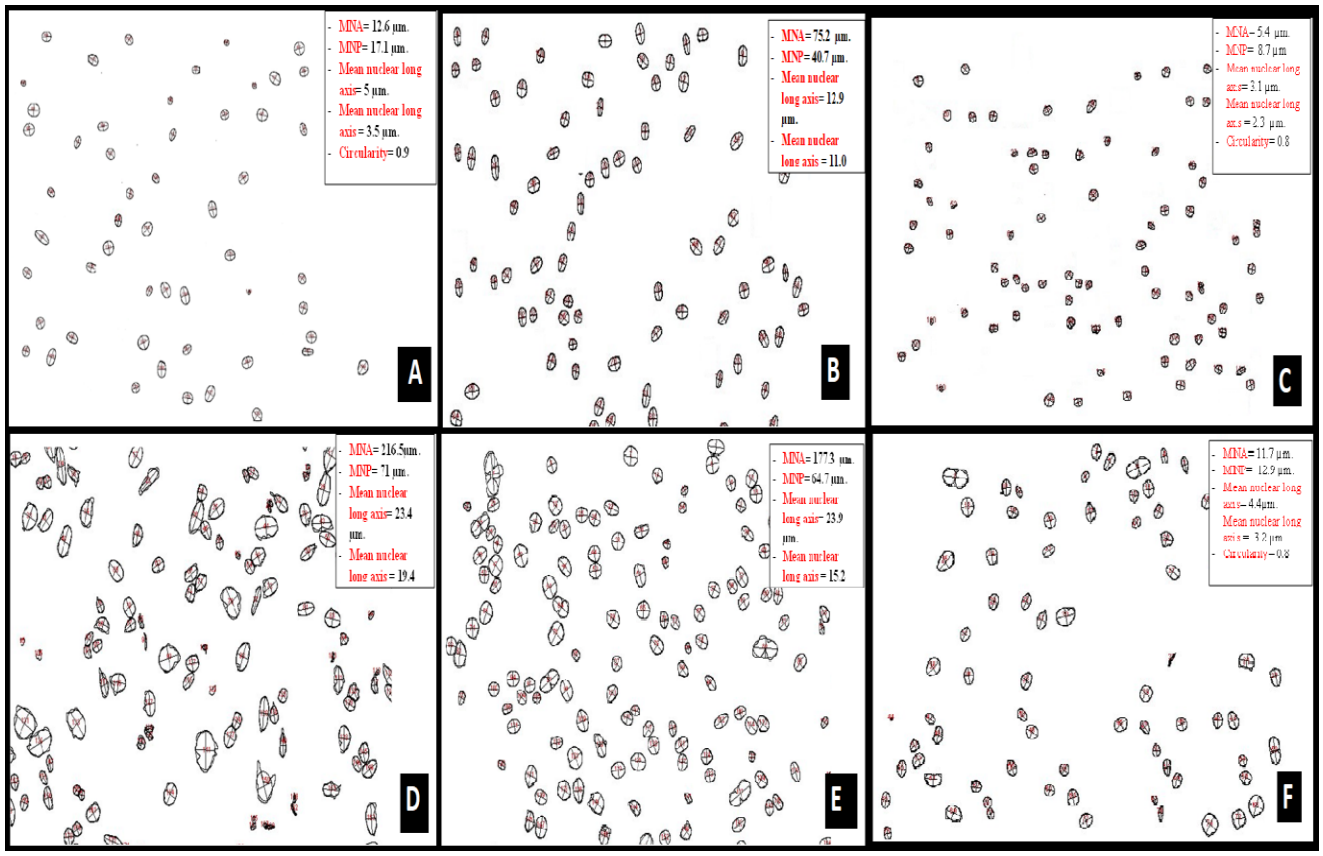

Figure 4: (A) Image analysis output "outlines" of the measured nuclei of grade 1 clear RCC (original magnification, x400). (B) Image analysis output "outlines" of the measured nuclei of grade 1 papillary RCC (original magnification, x400). (C) Image analysis output "outlines" of the measured nuclei of grade 1 chromophobe RCC (original magnification, x400). (D) Image nalysis output "outlines" of the measured nuclei of grade 4 clear RCC (original magnification, x400). (E) Image analysis output "outlines" of the measured nuclei of grade 3 papillary RCC (original magnification, x400). (F) Image analysis output "outlines" of the measured nuclei of grade 3 chromophobe RCC (original magnification, x400).

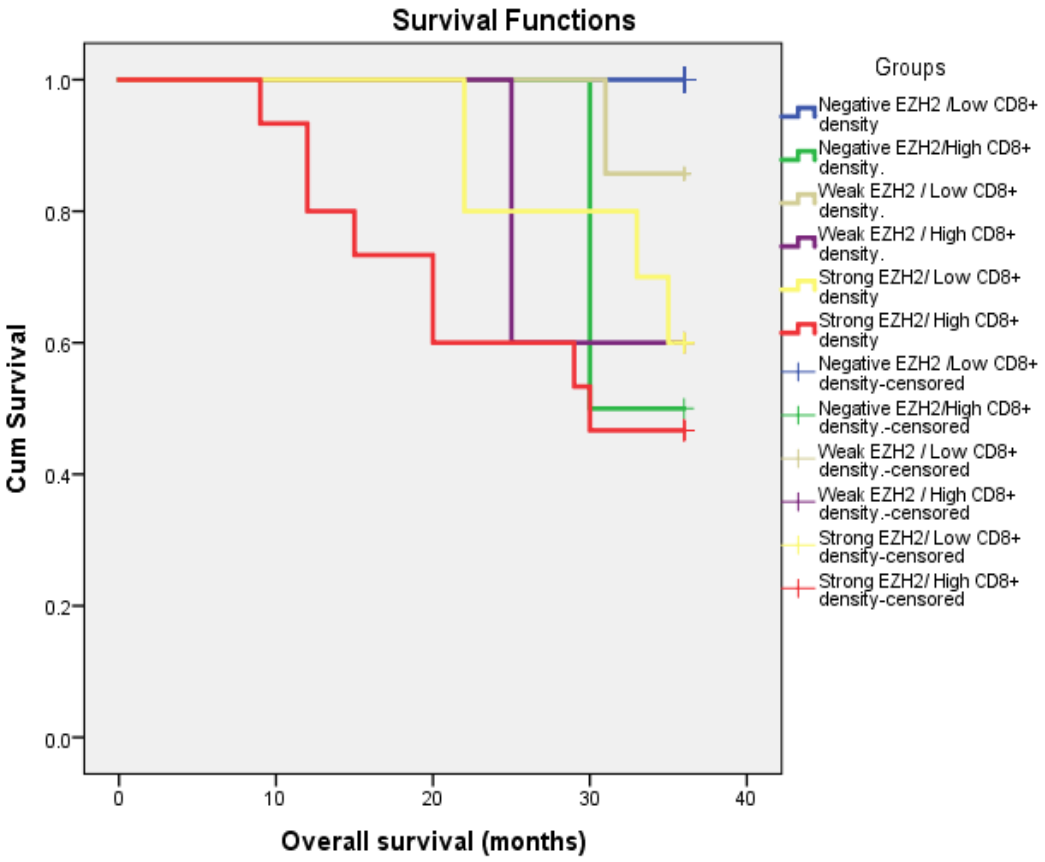

Figure (5) Kaplan–Meier estimates of the overall survival by combined EZH2 expression and CD8+ density.

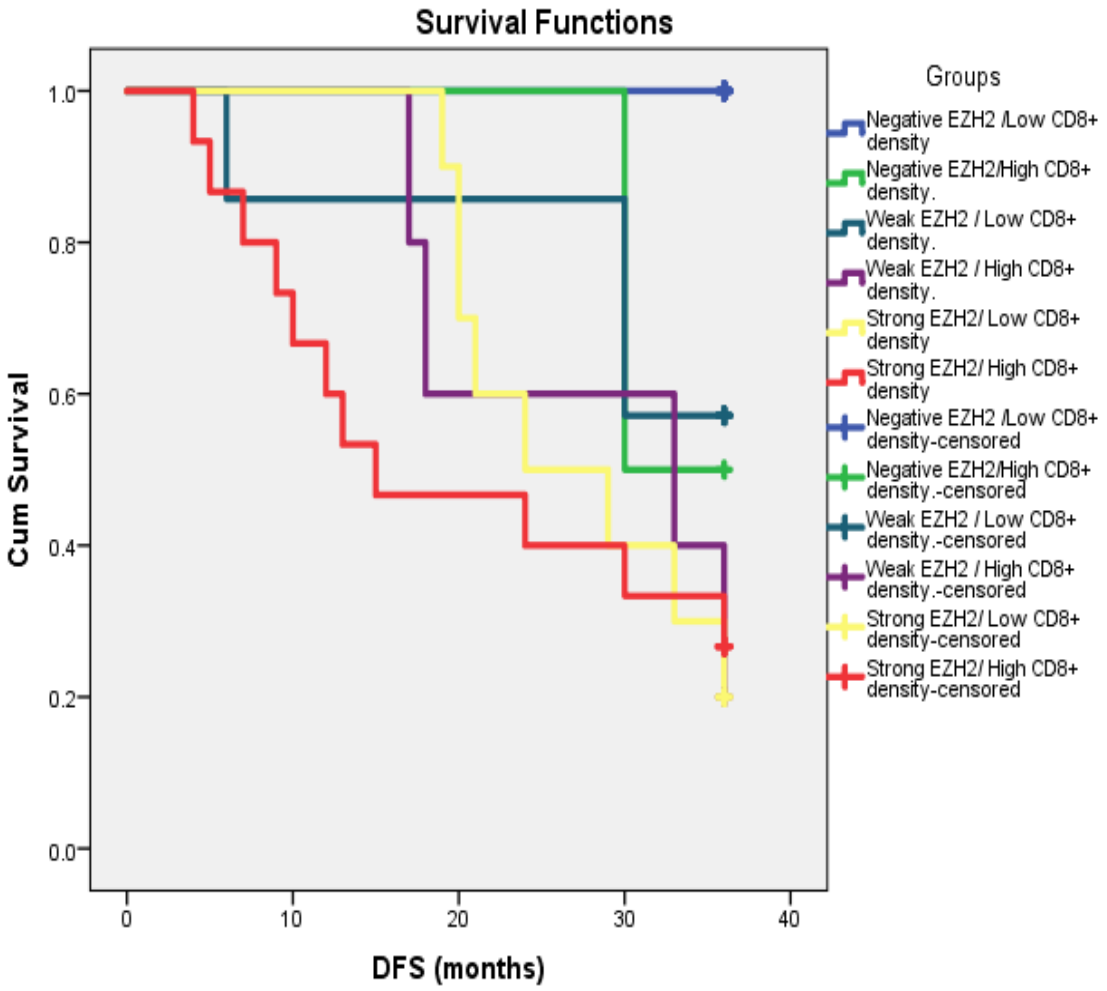

Figure (6) Kaplan–Meier estimates of the Disease-free survival by combined EZH2 expression and CD8+ density.

Table (1) Clinicopathological data of studied 55 RCC cases

Clinicopathological data of studied 55 RCC cases	
Gender	
Male	44 cases (80%)
Female	11 (20%)
Age	
Mean	55.47
Histologic type	
CCRCC	20 (36.4%)
PRCC	20 (36.4%)
ChRCC	15 ((27.3%)
Histologic Grade	
Grade 1	16 (29.1%)
Grade 2	23 (41.8%)
Grade 3	12 (21.8%)
Grade 4	4 (7.3%)
Primary tumor extent	
T1	26 (47.3%)
T2	22 (40%)
T3	7 (12.7%)
Nodal metastasis	
N0	38 (69.1%)
N1	17 (30.9%)
Distant metastasis	
M0	50 (90.9%)
M1	5 (9.1%)
AJCC stage group	
Stage I	22 (40%)
Stage II	15 (27.3%)
Stage III	16 (29.1%)
Stage IV	2 (3.6%)
overall survival	
Alive	39 (70.9%)
Died	16 (29.1%)
disease-free survival	
Free	28 (50.9%)
Recurrence/metastasis/ death	27 (49.1%)

*****CCRCC: clear cell renal cell carcinoma, PRCC: papillary renal cell carcinoma, ChRCC: chromophobe renal cell carcinoma .

Table (2).Relation of EZH2 IHC with pathological features of studied RCC cases:

		N	EZH2 IHC Expression			P-value
			Negative	Weak	Strong	
RCC subtype	CCRCC (%)	20	7 (35%)	3 (15%)	10 (50%)	0.731
	PRCC (%)	20	5 (25%)	5 (25%)	10 (50%)	
	ChRCC (%)	15	6 (40%)	4 (26.7%)	5 (33.3%)	
Histologic grade	Grade 1 (%)	16	12 (75%)	1 (6.3%)	3 (18.7%)	0.002*
	Grade 2 (%)	23	5 (21.7%)	6 (26.1%)	12 (52.2%)	
	Grade 3 (%)	12	1 (8.3%)	4 (33.3%)	7 (58.4%)	
	Grade 4 (%)	4	0 (0%)	1 (25%)	3 (75%)	
Primary tumor extent	T1 (%)	26	١٣ (٥٠%)	7 (٢٦.٩%)	6 (23.1%)	٠.012*
	T2 (%)	22	4 (18.2%)	٥ (22.7%)	1٣ (59.1%)	
	T3 (%)	7	١ (14.3%)	0 (0%)	٦ (85.7%)	
Nodal metastasis	N0 (%)	38	١٦ (42.1%)	٩ (23.7%)	1٣ (34.2%)	٠.03٣*
	N1 (%)	17	٢ (11.8%)	٣ (17.6%)	١٢ (70.6%)	
Distant Metastasis	M0 (%)	50	1٨ (٣٦%)	١٢ (٢٤%)	20 (٤٠%)	0.044*
	M1 (%)	5	0 (0%)	0 (0%)	٥ (100%)	
AJCC stage group	Stage I (%)	22	١٢ (54.5%)	٧ (٣1.8%)	٣ (1٣.٦%)	٠.004**
	Stage II (%)	15	4 (26.7%)	2 (13.3%)	9 (60%)	
	Stage III (%)	16	٢ (١2.5%)	٣ (18.8%)	١١(68.8%)	
	Stage IV (%)	2	0 (0%)	0 (0%)	2 (100%)	
CD8+ density	Low density (%)	33	16 (48.5%)	7 (21.2%)	10 (30.3%)	0.005**
	High density (%)	22	2 (9.1%)	5 (22.7%)	15 (86.2%)	
Overall survival	Alive (%)	39	17 (43.6%)	9 (23.1%)	13 (33.3%)	0.009**
	Dead (%)	16	1 (6.3%)	3 (18.8%)	12 (75%)	
Disease-free survival	Free (%)	28	17 (60.7%)	5 (17.9%)	6 (21.4%)	<0.001**
	Diseased/ died (%)	27	1 (3.7%)	7 (25.9%)	19 (70.4%)	
Total		55	18	12	25	

N: Number, *: Significant, **: Highly significant, CCRCC: clear cell renal cell carcinoma, PRCC: papillary renal cell carcinoma, ChRCC: chromophobe renal cell carcinoma, EZH2: Enhancer of zeste- homolog 2.

Table (3) Relation between CD8+ density and pathological features of studied RCC cases:

		N	CD8+ density		P-value
			Low density	High density	
RCC subtype	**CCRCC (%)**	**20**	**6 (30%)**	**14 (70%)**	**<0.001****
	PRCC (%)	**20**	**12 (60%)**	**8 (40%)**	
	ChRCC (%)	**15**	**15 (100%)**	**0 (0%)**	
Histologic grade	**Grade 1 (%)**	**16**	**16 (100%)**	**0 (0%)**	**<0.001****
	Grade 2 (%)	**23**	**14 (60.9%)**	**9 (39.1%)**	
	Grade 3 (%)	**12**	**3 (25%)**	**9 (75%)**	
	Grade 4 (%)	**4**	**0 (0%)**	**4 (100%)**	
Primary tumor extent	**T1 (%)**	**26**	**21(80.8%)**	**5 (19.2%)**	**<0.001****
	T2 (%)	**22**	**12 (54.5%)**	**10 (45.5%)**	
	T3 (%)	**7**	**0 (0%)**	**7 (100%)**	
Nodal metastasis	**N0 (%)**	**38**	**28 (73.7%)**	**10 (26.3%)**	**0.003****
	N1 (%)	**17**	**5 (29.4%)**	**12 (70.6%)**	
Distant metastasis	**M0 (%)**	**50**	**31 (62%)**	**19 (38%)**	**0.311**
	M1 (%)	**5**	**2 (40%)**	**3 (60%)**	
AJCC stage group	**Stage I (%)**	**22**	**19 (86.4%)**	**3 (13.6%)**	**0.001****
	Stage II (%)	**15**	**9 (60%)**	**6 (40%)**	
	Stage III (%)	**16**	**5 (31.3%)**	**11 (68.8%)**	
	Stage IV (%)	**2**	**0 (0%)**	**2 (100%)**	
EZH2 IHC Expression	**Negative**	**18**	**16 (88.9%)**	**2 (11.1%)**	**0.005****
	Weak	**12**	**7 (58.3%)**	**5 (41.7%)**	
	Strong	**25**	**10 (40%)**	**15 (60%)**	
Overall survival	**Alive (%)**	**39**	**28 (71.8%)**	**11 (28.2%)**	**0.005****
	Dead (%)	**16**	**5 (31.2%)**	**11 (68.8%)**	
Disease-free survival	**Free (%)**	**28**	**22 (78.6%)**	**6 (21.4%)**	**٠.004****
	Diseased/ died (%)	**27**	**11 (40.7%)**	**16 (59.3%)**	
Total			**33**	**22**	

N: Number, **: Highly significant, CCRCC: clear cell renal cell carcinoma, PRCC: papillary renal cell carcinoma, ChRCC: chromophobe renal cell carcinoma

Table (4) Relation between combined (EZH2 expression and CD8+ density), the overall survival, and the disease-free survival.

	N	Overall survival		Log Rank test		Disease-free survival		Log Rank test	
		Alive	Dead	χ 2	P-value	Free	Diseased or died	χ 2	P-value
Negative EZH2 /Low CD8+ density	16	16 (100%)	0 (0%)	14.11	٠.015	16 (100%)	0 (0%)	23.36	<0.001
Negative EZH2/High CD8+ density.	2	1 (50%)	1 (50%)			1 (50%)	1 (50%)		
Weak EZH2 / Low CD8+ density.	7	6 (85.7%)	1 (14.3%)			4 (57.1%)	3 (42.9%)		
Weak EZH2 / High CD8+ density.	5	3 (60%)	2 (40%)			1 (20%)	4 (80%)		
Strong EZH2/ Low CD8+ density	10	6(60%)	4 (40%)			2 (20%)	8 (80%)		
Strong EZH2/ High CD8+ density	15	7 (46.7%)	8 (53.3%)			4 (26.7%)	11 (73.3%)		
Total	55	39	16			28	27		

N: Number, χ 2:Chi-square test, EZH2: Enhancer of zeste- homolog 2.

Table (5) Relation of nuclear morphometric variables with some pathological features of studied cases

		N	MNA (μm^2)	MNP (µm)	MN long axis (µm)	MN short axis (µm)	Circularity
			Mean (±SD)	**Mean (±SD)**	**Mean (±SD)**	**Mean (±SD)**	**Mean (±SD)**
RCC subtype	**CCRCC**	20	88.6 (±92.6)	44.9 (±23.2)	14.1 (±7.5)	9.8 (±7)	0.7 (±0.2)
	PRCC	20	140.5 (±81.8)	55.5 (±15.3)	18.2 (±5.8)	13.9 (±3.7)	0.8 (±0.1)
	ChRCC	15	7.6 (±2.9)	10.2 (±2.2)	3.6 ± (0.7)	2.7 (±0.6)	0.9 (±0.03)
Histologic grade	**Grade 1**	16	**28.1 (±33.3)**	**20.2 (±14.9)**	**6.8 (±4.7)**	**5.3 (±4)**	**0.9 (±0.08)**
	Grade 2	23	**73.7 (±85.3)**	**40.4 (±21.9)**	**12.6 (±7.3)**	**8.4 (±5.2)**	**0.7 (±0.2)**
	Grade 3	12	**136.6 (±93.8)**	**50.4 (±24.7)**	**17 (±8.4)**	**13.1 (±6.7)**	**0.8 (±0.06)**
	Grade 4	4	**227.3 (±17.7)**	**75.4 (±6)**	**24.3 (±1.2)**	**20.2 (±2.2)**	**0.8 (±0.05)**
Tumor extent	**T1**	26	**49.9 (±53.8)**	**29.3 (±19.9)**	**9.4 (±6)**	**7 (±5)**	0.8 (±0.1)
	T2	22	**94.9 (±91.8)**	**42.7 (±25.8)**	**14 (±8.9)**	**9.9 (±6.6)**	0.8 (±0.18)
	T3	7	**186.9 (±119.4)**	**65.3 (±17.6)**	**21 (±6.2)**	**16.3 (±6.7)**	0.7 (±0.2)
Nodal metastasis	**N0**	38	**69 (±73.9)**	**34.3 (±22.5)**	**11.2 (±7.3)**	**8.2 (±5.5)**	0.8 (±0.16)
	N1	17	**121.8 (±113.7)**	**50.2 (±26.9)**	**16.2 (±9)**	**12 (±7.8)**	0.7 (±0.18)
Distant metastasis	**M0**	50	**77.8 (±84.1)**	**37.2 (±23.6)**	**12 (±7.8)**	**8.8 (±6.1)**	0.8 (±0.17)
	M1	5	**161 (±126.2)**	**60.2 (±29.9)**	**20 (±9.5)**	**15.1 (±7.8)**	0.7 (±0.18)
AJCC stage group	**Stage I**	22	**58.9 (±56.3)**	**31.4 (±20.5)**	**10.1 (±6.3)**	**7.9 (±5.2)**	0.8 (±0.1)
	Stage II	15	**67.2 (±71)**	**35.5 (±22.8)**	**11.7 (±8.2)**	**7.7 (±5.4)**	0.8 (±0.2)
	Stage III	16	**119.6 (±120.8)**	**48.6 (±27)**	**15.7 (±9)**	**11.3 (±7.4)**	0.7 (±0.18)
	Stage IV	2	**238.4 (±21.1)**	**79.7 (±5.9)**	**25.1 (±1.3)**	**21.9 (±0.2)**	0.8 (±0.07)
Total cases (N=55)			85.3 (90.5)	39.3 (24.8)	12.7 (8)	9.4 (6.5)	.78 (0.16)

Bold values are significant.

N: Number, MNA: Mean nuclear area, MNP: Mean nuclear perimeter, CCRCC: clear cell renal cell carcinoma, PRCC: papillary renal cell carcinoma, ChRCC: chromophobe renal cell carcinoma.

Table (6) Relation of nuclear morphometric variables with EZH2 expression, CD8+ density and with survival in studied cases

		N	MNA (μm^2)	MNP (µm)	MN long axis (µm)	MN short axis (µm)	Circularity
			Mean (±SD)	**Mean (±SD)**	**Mean (±SD)**	**Mean (±SD)**	**Mean (±SD)**
EZH2 IHC Expression	**Negative**	18	**38.2 (±46.8)**	**26.6 (±19.9)**	**8.3 (±5.7)**	**6.2 (±4.9)**	0.77 (±0.2)
	Weak	12	**83.2 (±71.8)**	**38.4 (±21.6)**	**12.3 (±6.8)**	**9.9 (±5.6)**	0.8 (±0.15)
	Strong	25	**120.2 (±107.5)**	**48.8 (±26)**	**16.1 (±8.8)**	**11.4 (±7.1)**	0.77 (±0.16)
CD8+ density	**Low density**	33	**45.8 (±61.8)**	**26.6 (±21.3)**	**8.7 (±7)**	**6.4 (±4.8)**	0.8 (±0.14)
	High density	22	**144.6 (±95.4)**	**58.3 (±16.3)**	**18.7 (±5.8)**	**13.8 (±6.2)**	0.71 (±0.18)
Overall survival	**Alive**	**39**	**56.668(± 68.9)**	**32.081 (± 21.3)**	**10.290 (± 6.7)**	**7.277 (±5)**	**0.777 (± 0.18)**
	Dead	**16**	**155.240 (±100.4)**	**56.751 (±24.6)**	**18.694 (±8.4)**	**14.444 (±6.8)**	**0.777 (± 0.18)**
Disease-free survival	**Free**	28	**47.8 (±103)**	**30.3 (±20.3)**	**9.6 (±6.4)**	**6.7 (±4.7)**	0.77 (±0.18)
	Diseased/ died	27	**124.3 (±103.1)**	**48.6 (±26)**	**16 (±8.6)**	**12.1 (±7)**	0.78 (±0.16)
Total cases (N=55)			85.3 (90.5)	39.3 (24.8)	12.7 (8)	9.4 (6.5)	.78 (0.16)

-**Bold values** are significant.

N: Number, MNA: Mean nuclear area, MNP: Mean nuclear perimeter, EZH2: Enhancer of zeste- homolog

There was highly significant statistical difference between CD8+ density and MNA, MNP, mean nuclear long axis, and mean nuclear short axis (P <0.001, for each). No significant statistical difference was found between the mean nuclear circularity and EZH2 expression(P=0.598), or CD8+ density(P= 0.056). A highly significant inverse statistical correlation was found between the OS and MNA, MNP, mean nuclear long axis, and mean nuclear short axis (P<0.001, for each). There was a highly significant inverse statistical correlation between the DFS and MNA (P =0.003), MNP (P=0.006), mean nuclear long axis (P=0.003), and mean nuclear short axis (P=0.00)

Discussion

EZH2 dysregulation is strongly correlated with poor prognosis of numerous types of cancer [21]. In our study, EZH2 immunostaining was detected in 67.3% of RCC cases. This finding was within the range of previous studies that reported EZH2 positivity in 44% [22],78% [23], and in 75.2% [24] of studied RCC cases. Different EZH2 expression levels among studies can be due to different selected antibodies and different immunostaining protocols.

In our study, there was a highly significant relation between EZH2 expression and histologic grade (P=0.002), tumor extent (P=0.012), nodal metastasis (P= 0.033), distant metastasis (P=0.044), and AJCC stage group (P=0.004). These results run parallel to previous studies that reported that EZH2 expression was related to advanced tumor stages, positive lymph nodes, distant metastases, and a higher nuclear grade in RCC [25-26-27-28-29]. This could be explained by EZH2 involvement in regulating cell cycle progression and that EZH2 dysregulation accelerates cell proliferation, leading to cancer development[30]. EZH2 also facilitates tumorigenesis through promoting angiogenesis[21]. On the other side, previous authors[31] demonstrated no significant relation of EZH2 expression with RCC grade, stage, or distant metastasis. This discrepancy can be owed to different sample sizes, different techniques of IHC staining and different assessment score of EZH2.

A highly significant relation was found between EZH2 expression and OS (P=0.008) and DFS (P <0.001). Increased EZH2 expression in RCC is associated with shortened patients' survival. These results are in line with previous studied [25-32-28]. This can be explained by the significant relation of EZH2 expression with the other adverse prognostic factors.

In contrast, other authors reported that patients with high EZH2 mRNA levels independently showed longer OS and DFS in RCC patients[33]. Such conflicting results may be due to different methods for assessing EZH2 expression.

In our study, no significant statistical difference was found between EZH2 IHC expression and RCC types in studied cases (P=0.731). This runs parallel with previous studies [26-28]. Other authors reported that EZH2 expression was highest in papillary RCC, followed by CCRCC, and least in chromophobe[24]. These different results could be due to different antibodies used and different sample size of studied cases.

High CD8+ T cell densities were found to be associated with a favorable prognosis in various solid tumors. However, the role of CD8+ lymphocytes in RCC is still controversial [34-35].

CD8+ density in studied cases ranged from 13 to 1001 cells/mm2 with a mean of 257.35 cells/mm2. Previous studies reported a mean CD8+ density of 342 cells/mm2 [24] and 649 cells/mm2 [36]. These differences could be attributed to different number of cases and different algorithms for calculating CD8+ density. Our study highlighted a significant relation between the mean CD8+ density and RCC subtypes (P <0.001). The mean CD8+ density was highest in CCRCC (476.20 cells/mm2), and least in ChRCC (29.60 cells/mm2). The finding of low CD8+ infiltration in ChRCC might be a contributing factor for its known poor

response to immunotherapy, compared to CCRCC[37].

We used the sample median CD8+ density (184 cells/mm2) as a cut-off point to separate low, from high CD8+ density[19]. A highly significant relation was found between CD8+ density and the histologic type of RCC (P= 0.0001). these results were in agreement with previous studies [38-34-39].

There was a highly significant relation between CD8+ density and the histologic grade in studied RCC cases (P<0.001). These results are in line with previous studies in RCC [40-38]. Previous authors reported that high CD8+ infiltration is related to higher histologic grades in non-small cell lung cancer[41]. This could be explained by the fact that the more dedifferentiated cancers express increased amounts of tumor-associated antigens that are recognized by T cells and be recruited in cancer tissue. In contrast, other studies found higher CD8+ infiltration in the well-differentiated tumors than poorly-differentiated ones[42]. This discrepancy could be due to different RCC subtypes studied and tumor immunologic heterogenicity.

In our study, a highly significant relation was found between CD8+ density and the tumor extent (P<0.001), nodal metastasis (P= 0.003), and the AJCC stage (P= 0.001). Similarly, previous authors found that high CD8+ count was significantly associated with advanced tumor stage (p =0.004) and distant metastasis (p= 0.002) [24]. This could be explained by the fact that effector CD8+ cells show enhanced proliferation under hypoxic conditions, mediated by metabolic changes in the advanced tumors[43]. In contrast, other study reported no association of infiltrating CD8+ lymphocytes and tumor stage, nodal or distant metastasis in RCC[44]. Another study reported that lower CD8+ infiltration was associated with large tumor size, and higher stage in hepatocellular carcinoma[45]. This discrepancy could be explained by different tissues or intratumoral immunologic heterogeneity.

In our work, a highly significant relation was found between CD8+density and OS (P=0.001), and DFS (P=0.001); denoting poor prognosis associated with the high CD8+density. Similarly, previous studies demonstrated that high CD8+ infiltration is linked to shorter survival of the patients in RCC[46-47-48]. These results are different from other solid malignancies, in which increased CD8+ T cell infiltration is associated with a favorable prognosis and prolonged survival[49-50].

According to our results, CD8+ infiltration into RCC does not constitute anti-tumor immune response. This could be owed to T-cell exhaustion that occurs in advanced stage and high grade RCCs, which is linked to high CD8+ density[34].

In contrast to the poor prognostic evidence of CD8+ density, Some studies found that higher CD8+ T cell infiltration is associated with better overall and cancer specific survival in RCC [51-52-53-54]. This conflict among studies can be explained by different study design and different follow-up time. Different techniques of CD8+ assessment in tissues, and different adopted cut-off value for defining high CD8+ tumors.

Our study showed a highly significant relation between EZH2 expression and CD8+ density (P= 0.005). Previous studies revealed that number of CD8+ cells

increased with raising EZH2 levels in RCC cases [24-55-49]. So, it is suggested that lymphocytic infiltration might cause strong EZH2 overexpression in RCC and the resulting immune evasion could explain the unique association between high density of CD8+ cells in RCC and unfavorable outcome which is different from most solid cancers.

In this work, a significant relation was found between the six groups of combined EZH2 expression and CD8+ density, with patient survival. Negative EZH2 /Low CD8+ density group was associated with the most prolonged OS and DFS than other groups. These results support that EZH2 worse prognosis is linked to the increase of CD8+ density, suggesting the vulnerability of tumors harboring EZH2 expression to immunotherapy.

Digital nuclear morphology is a less subjective and more precise method for detecting nuclear criteria[18]. In our study, nuclear morphometric results, were close to previous studies in literature [56-13]. Different values among RCC subtypes can be explained by different molecular events of each subtype progression [57].

The MNA, MNP, mean nuclear long axis and mean nuclear short axis showed a significant relation with the histologic grade (P<0.001, for each), tumor extent (P= 0.001, 0.001, 0.001, and 0.002 respectively), nodal metastasis (P= 0.044, 0.027, 0.032, and 0.038 respectively), distant metastasis (P= 0.049, 0.047, 0.036, and 0.037 respectively), and AJCC stage group (P= 0.011, 0.013, 0.022, and 0.009 respectively). These results run parallel to previous studies [58-56-59-13] .

There was a significant statistical relation between EZH2 expression in RCC and MNA (P= 0.011), MNP (P= 0.013), and mean nuclear short axis (P= 0.027), and a highly significant relation with the mean nuclear long axis (P= 0.006). This could be owed to the forementioned relation of both nuclear morphometric parameters and EZH2 expression, with adverse clinicopathological parameters.

There was a highly significant difference between CD8+ density in RCC and MNA, MNP, mean nuclear long axis, and mean nuclear short axis (P <0.001, for each). This result could be on basis that CD8+ density in our work is related to adverse clinicopathological variables , which in turn correlates with higher nuclear morphometry values.

As regard to patients' survival, a highly significant inverse correlation was found between OS in RCC and MNA, MNP, mean nuclear long axis, and mean nuclear short axis (P<0.001, for each). Regarding the DFS, there was a highly significant inverse correlation between DFS in RCC and MNA (P =0.003), MNP (P=0.006), mean nuclear long axis (P=0.003), and mean nuclear short axis (P=0.002). These results run parallel to previous studies [58-56-59-13] that reported strong inverse correlation of MNA, MNP, mean nuclear long axis and mean nuclear short axis values with the patient survival in RCC.

Conclusion

This study seems to be the first in literature discussing the relation between EZH2 expression , CD8+ density and nuclear morphometric parameters in RCC till date. EZH2 and CD8+ could be reliable

prognostic biomarkers in RCC. Supporting them with nuclear morphometric data could aid in risk stratification of cases. Further studies on a large scale are needed to support these findings.

References

1. **Bahadoram S, Davoodi M, Hassanzadeh S, Bahadoram M, Barahman M, Mafakher L**. Renal cell carcinoma: an overview of the epidemiology, diagnosis, and treatment. G Ital Nefrol. 2022;39(3).
2. **Sung H, Ferlay J, Siegel RL, Laversanne M, Soerjomataram I, Jemal A, et al.** Global Cancer Statistics 2020: GLOBOCAN Estimates of Incidence and Mortality Worldwide for 36 Cancers in 185 Countries. CA Cancer J Clin. 2021;71(3):209–49.
3. **Sharma A, Narayanasamy K, Murugesan A, Madhavan D**. Clinicopathological Spectrum of Renal Tumors in Tamil Nadu. 2024;5–7.
4. **Jani KS, Jain SU, Ge EJ, Diehl KL, Lundgren SM, Müller MM, et al.** Histone H3 tail binds a unique sensing pocket in EZH2 to activate the PRC2 methyltransferase. Proc Natl Acad Sci. 2019;116(17):8295–300.
5. **Gan L, Yang Y, Li Q, Feng Y, Liu T, Guo W**. Epigenetic regulation of cancer progression by EZH2: from biological insights to therapeutic potential. Biomark Res. 2018;6(1):1–10.
6. **Zhang T, Gong Y, Meng H, Li C, Xue L**. Symphony of epigenetic and metabolic regulation—interaction between the histone methyltransferase EZH2 and metabolism of tumor. Clin Epigenetics. 2020;12(1):1–15.
7. **Kumari R, Jat P**. Mechanisms of cellular senescence: cell cycle arrest and senescence associated secretory phenotype. Front cell Dev Biol. 2021;9:485.
8. **Wu J, Sun L, Liu T, Dong G**. Ultrasound-targeted microbubble destruction-mediated downregulation of EZH2 inhibits stemness and epithelial-mesenchymal transition of liver cancer stem cells. Onco Targets Ther. 2021;221–37.
9. **Huang J, Gou H, Yao J, Yi K, Jin Z, Matsuoka M, et al.** The noncanonical role of EZH2 in cancer. Cancer Sci. 2021;112(4):1376–82.
10. **Bharadwaj S, Kirtipal N, Sobti RC**. Recent Developments in the Immunotherapeutic Approaches for Cancer Treatment. Biomed Transl Res From Dis Diagnosis to Treat. 2022;413–49.
11. **Guo C, Zhao H, Wang Y, Bai S, Yang Z, Wei F, et al.** Prognostic value of the neo-immunoscore in renal cell carcinoma. Front Oncol. 2019;9(MAY):1–13.
12. **Rabjerg M, Gerke O, Engvad B, Marcussen N**. Comparing World Health Organization/International Society of Urological Pathology Grading and Fuhrman Grading with the Prognostic Value of Nuclear Area in Patients with Renal Cell Carcinoma. Uro. 2021;1(1):2–13.
13. **Agrawal S, Jain N**. Nuclear Morphometry is a superior Prognostic Predictor in comparison to Histological grading in Renal cell Carcinoma: A Retrospective Clinico-pathological study. Indian J Pathol Oncol. 2022;52(1–2):1–3.
14. **Kim KH, Roberts CWM**. Targeting EZH2 in cancer. Nat Med. 2016;22(2):128–34.
15. **Vagios S, Yiannou P, Giannikaki E, Doulgeraki T, Papadimitriou C, Rodolakis A, et al.** The impact of programmed cell death-ligand 1 (PD-L1) and CD8 expression in grade 3 endometrial carcinomas. Int J Clin Oncol. 2019;24:1419–28.
16. **Samal S, Patnaik A, Sahu FM, Purkait S**. Altered expression of epigenetic modifiers EZH2, H3K27me3, and DNA methyltransferases in meningiomas-Prognostic biomarkers for routine practice. Folia Neuropathol. 2020;58(2):133–42.
17. **Schneider CA, Rasband WS, Eliceiri KW**. NIH Image to ImageJ: 25 years of image analysis. Nat Methods. 2012;9(7):671–5.
18. **Crowe AR, Wei Y**. Semi-quantitative Determination of Protein Expression Using Immunohistochemistry Staining and Analysis.

Bio-protocol. 2019;9(24):1–11.

19. **Glaire MA, Domingo E, Sveen A, Bruun J, Nesbakken A, Nicholson G, et al.** Tumour-infiltrating CD8+ lymphocytes and colorectal cancer recurrence by tumour and nodal stage. Br J Cancer. 2019;(July).

20. **Raghavan V, Rao KR**. An ImageJ Based Semi-Automated Morphometric Assessment of Nuclei in Oncopathology. Int J Sci Study. 2015;3(7):189–94.

21. **Gao J, Fosbrook C, Gibson J, Underwood TJ, Gray JC, Walters ZS**. Review: Targeting EZH2 in neuroblastoma. Cancer Treat Rev. 2023;119(July):1–8.

22. **Sakurai T, Bilim VN, Ugolkov A V, Yuuki K, Tsukigi M, Motoyama T, et al.** The enhancer of zeste homolog 2 (EZH2), a potential therapeutic target, is regulated by miR-101 in renal cancer cells. Biochem Biophys Res Commun. 2012;422(4):607–14.

23. **Wang Y, Chen Y, Geng H, Qi C, Liu Y, Yue D**. Overexpression of YB1 and EZH2 are associated with cancer metastasis and poor prognosis in renal cell carcinomas. Tumor Biol. 2015;36(9):7159–66.

24. **Eichenauer T, Simmendinger L, Fraune C, Mandelkow T, Blessin NC, Kluth M, et al.** High level of EZH2 expression is linked to high density of CD8-positive T-lymphocytes and an aggressive phenotype in renal cell carcinoma. World J Urol. 2021;39(2):481–90.

25. **Wagener N, Macher-Goeppinger S, Pritsch M, Hüsing J, Hoppe-Seyler K, Schirmacher P, et al.** Enhancer of zeste homolog 2 (EZH2) expression is an independent prognostic factor in renal cell carcinoma. BMC Cancer. 2010;10.

26. **Tian Y, Hong M, Guo Q, Chen Z, Jing S, Ma B, et al.** Clinicopathological and prognostic relevance of EZH2 expression in renal cell carcinoma: A meta-analysis. Int J Clin Exp Med. 2016;9(6):9714–24.

27. **Sun C, Zhao C, Li S, Wang J, Zhou Q, Sun J, et al.** EZH2 Expression is increased in BAP1-mutant renal clear cell carcinoma and is related to poor prognosis. J Cancer. 2018;9(20):3787.

28. **Bai YK, Sun J, Wang YS, Zheng N, Xu Q Le, Wang Y**. The clinicopathological and prognostic significances of EZH2 expression in urological cancers: A meta-analysis and bioinformatics analysis. Oncol Lett. 2023;26(1):1–11.

29. **Xu S, Ma B, Feng X, Yao C, Jian Y, Chen Y, et al.** EZH2-regulated immune risk score prognostic model predicts outcome of clear cell renal cell carcinoma. Transl Androl Urol. 2023;12(1):71–82.

30. **Raspin K, FitzGerald LM, Marthick JR, Field MA, Malley RC, Banks A, et al.** A rare variant in EZH2 is associated with prostate cancer risk. Int J Cancer. 2021;149(5):1089–99.

31. **Hinz S, Weikert S, Magheli A, Hoffmann M, Engers R, Miller K, et al.** Expression Profile of the Polycomb Group Protein Enhancer of Zeste Homologue 2 and its Prognostic Relevance in Renal Cell Carcinoma. J Urol. 2009;182(6):2920–5.

32. **Liu L, Xu Z, Zhong L, Wang H, Jiang S, Long Q, et al.** Enhancer of zeste homolog 2 (EZH2) promotes tumour cell migration and invasion via epigenetic repression of E-cadherin in renal cell carcinoma. BJU Int. 2016;117(2):351–62.

33. **Lee HW, Choe M**. Expression of EZH2 in renal cell carcinoma as a novel prognostic marker. Pathol Int. 2012;62(11):735–41.

34. **Chandrasekaran D, Td B, Sundaram S**. TUMOR INFILTRATING CD8 LYMPHOCYTES IN ADVANCED RENAL CELL CARCINOMA CASES – AN IMMUNOHISTOCHEMISTRY STUDY. 2023;1036–41.

35. **Beck JD, Diken M, Suchan M, Streuber M, Diken E, Kolb L, et al.** Long-lasting mRNA-encoded interleukin-2 restores CD8+ T cell neoantigen immunity in MHC class I-deficient cancers. Cancer Cell. 2024;

36. **Blessin NC, Li W, Mandelkow T, Jansen HL, Yang C, Raedler JB, et al.** Prognostic role of proliferating CD8+ cytotoxic Tcells in human cancers. Cell Oncol. 2021;44(4):793–803.

37. **Alchoueiry M, Labaki C, Zhang L, Hou Y, Bi K, Hobeika C, et al.** Abstract B019: Clinical

and molecular characterization of chromophobe renal cell carcinoma: A focus on immunotherapy based regimens and the tumor immune microenvironment. Cancer Res. 2023;83(16_Supplement):B019–B019.

38. **Murakami T, Tanaka N, Takamatsu K, Hakozaki K, Fukumoto K, Masuda T, et al.** Multiplexed single-cell pathology reveals the association of CD8 T-cell heterogeneity with prognostic outcomes in renal cell carcinoma. Cancer Immunol Immunother. 2021;70(10):3001–13.

39. **Labaki C, Alchoueiry M, Bi K, Zhang L, Hobeika C, Bakouny Z, et al.** Cellular and molecular determinants of limited anti-tumor immunity in chromophobe renal carcinoma (ChRCC). American Society of Clinical Oncology; 2024.

40. **Kawashima A, Kanazawa T, Kidani Y, Yoshida T, Hirata M, Nishida K, et al.** Tumour grade significantly correlates with total dysfunction of tumour tissue-infiltrating lymphocytes in renal cell carcinoma. Sci Rep. 2020;10(1):1–13.

41. **Schulze AB, Evers G, Görlich D, Mohr M, Marra A, Hillejan L, et al.** Tumor infiltrating T cells influence prognosis in stage I–III non-small cell lung cancer. J Thorac Dis. 2020;12(5):1824.

42. **Hamad AS m**. Characterization of immune cell infiltration in clear cell renal cell carcinoma Almotasem Salah-M Hamad. 2024;

43. **Liikanen I, Lauhan C, Quon S, Omilusik K, Phan AT, Bartrolí LB, et al.** Hypoxia-inducible factor activity promotes antitumor effector function and tissue residency by CD8+ T cells. J Clin Invest. 2021;131(7).

44. **Eich ML, Athar M, Ferguson JE, Varambally S**. EZH2-targeted therapies in cancer: Hype or a reality. Cancer Res. 2020;80(24):5449–58.

45. **Xu X, Tan Y, Qian Y, Xue W, Wang Y, Du J, et al.** Clinicopathologic and prognostic significance of tumor-infiltrating CD8+ T cells in patients with hepatocellular carcinoma: A meta-analysis. Med (United States). 2019;98(2).

46. **Nakano O, Naito Y, Nagura H, Ohtani H, Nakano O, Sato M, et al.** Proliferative activity of intratumoral CD8+ T-lymphocytes as a prognostic factor in human renal cell carcinoma: Clinicopathologic demonstration of antitumor immunity. Cancer Res. 2001;61(13):5132–6.

47. **Giraldo NA, Becht E, Vano Y, Petitprez F, Lacroix L, Validire P, et al.** Tumor-infiltrating and peripheral blood T-cell immunophenotypes predict early relapse in localized clear cell renal cell carcinoma. Clin Cancer Res. 2017;23(15):4416–28.

48. **Zhu Q, Cai MY, Weng DS, Zhao JJ, Pan QZ, Wang QJ, et al.** PD-L1 expression patterns in tumour cells and their association with CD8 + tumour infiltrating lymphocytes in clear cell renal cell carcinoma. J Cancer. 2019;10(5):1154–61.

49. **Tavana S, Mokhtari Z, Sanei MH, Heidari Z, Dehghanian AR, Faghih Z, et al.** Clinicopathological significance and prognostic role of LAG3 + tumor-infiltrating lymphocytes in colorectal cancer; relationship with sidedness. Cancer Cell Int. 2023;23(1):1–13.

50. **Yazaki S, Shimoi T, Yoshida M, Sumiyoshi-Okuma H, Arakaki M, Saito A, et al.** Integrative prognostic analysis of tumor–infiltrating lymphocytes, CD8, CD20, programmed cell death-ligand 1, and tertiary lymphoid structures in patients with early-stage triple-negative breast cancer who did not receive adjuvant chemotherapy. Breast Cancer Res Treat. 2023;197(2):287–97.

51. **Zhang S, Zhang E, Long J, Hu Z, Peng J, Liu L, et al.** Immune infiltration in renal cell carcinoma. Cancer Sci. 2019;110(5):1564–72.

52. **Jansen CS, Prokhnevska N, Master VA, Sanda MG, Carlisle JW, Bilen MA, et al.** An intra-tumoral niche maintains and differentiates stem-like CD8 T cells. Nature. 2019;576(7787):465–7

53. **Eich ML, Chaux A, Mendoza Rodriguez MA, Guner G, Taheri D, Rodriguez Pena MDC, et al.** Tumour immune microenvironment in primary and metastatic papillary renal cell carcinoma. Histopathology. 2020;76(3):423–32.

54. **Shapiro DD, Lozar T, Cheng L, Xie E, Laklouk I, Lee MH, et al.** Non-Metastatic Clear Cell Renal Cell Carcinoma Immune Cell Infiltration Heterogeneity and Prognostic Ability in Patients Following Surgery. Cancers (Basel). 2024;16(3).

55. **Lyu C, Wang L, Stadlbauer B, Noessner E, Buchner A, Pohla H**. Identification of EZH2 as Cancer Stem Cell Marker in Clear Cell Renal Cell Carcinoma and the Anti-Tumor Effect of Epigallocatechin-3-Gallate (EGCG). Cancers (Basel). 2022;14(17).

56. **Özer E, Yörükoğlu K, Sagol Ö, Mungan U, Demirel D, Tüzel E, et al.** Prognostic significance of nuclear morphometry in renal cell carcinoma. BJU Int. 2002;90(1):20–5.

57. **Kumar N, Verma R, Chen C, Lu C, Fu P, Willis J, et al.** Computer-extracted features of nuclear morphology in hematoxylin and eosin images distinguish s tage II and IV colon tumors. J Pathol. 2022;257(1):17–28.

58. **Val-Bernal JF**. Selective nuclear morphometry as a prognostic factor of survival in renal cell carcinoma. Histol Histopathol. 1999;14(1):119–23.

59. **Bektaş, Barut, Kertiş, Bahadir, Gün, Kandemir, et al.** Concordance of nuclear morphometric analysis with Fuhrman nuclear grade and pathologic stage in conventional renal cell carcinoma. Turkish J Pathol. 2008;24(1):14–8.

To cite this article: Eman M. Said, Ranih Z. Amer, Sara A. Madkour, Marwa S. Abd Allah. Assessment of (EZH2) Expression, Digital Image Analysis of CD8+ Lymphocytes, and Automated Nuclear Morphometry in Renal Cell Carcinoma. BMFJ 2024;41(6):164-185.